Journal of Cellular Biochemistry 64:547–564 (1997)

Bone Acidic Glycoprotein-75 Self-Associates to Form Macromolecular Complexes In Vitro and In Vivo with the Potential to Sequester Phosphate Ions

Jeffrey P. Gorski,[1]* Edward A. Kremer,[1] Yan Chen,[1] Steve Ryan,[1] Colleen Fullenkamp,[1] John Delviscio,[1] Karen Jensen,[2] and Marc D. McKee[3]

[1]Division of Molecular Biology and Biochemistry, School of Biological Sciences, University of Missouri–KC, Kansas City, Missouri
[2]Department of Biology and NIH Developmental Studies Hybridoma Bank, University of Iowa, Iowa City, Iowa
[3]Laboratory for Electron Microscopy, Department of Stomatology, Faculty of Dentistry, Université de Montréal, Montreal, Canada

Abstract Monoclonal antibody HTP IV-#1 specifically recognizes a complexation-dependent neoepitope on bone acidic glycoprotein-75 (BAG-75) and a Mr = 50 kDa fragment. Complexes of BAG-75 exist in situ, as shown by immunofluorescent staining of the primary spongiosa of rat tibial metaphysis and osteosarcoma cell micromass cultures with monoclonal antibody HTP IV-#1. Incorporation of BAG-75 into complexes by newborn growth plate and calvarial tissues was confirmed with a second, anti-BAG-75 peptide antibody (#503). Newly synthesized BAG-75 immunoprecipitated from mineralizing explant cultures of bone was present entirely in large macromolecular complexes, while immunoprecipitates from monolayer cultures of osteoblastic cells were previously shown to contain only monomeric Mr = 75 kDa BAG-75 and a 50 kDa fragment. Purified BAG-75 self-associated in vitro to form large spherical aggregate structures composed of a meshwork of 10 nm diameter fibrils. These structures have the capacity to sequester large amounts of phosphate ions as evidenced by X-ray microanalysis and by the fact that purified BAG-75 preparations, even after extensive dialysis against water, retained phosphate ions in concentrations more than 1,000-fold higher than can be accounted for by exchange calculations or by electrostatic binding. The ultrastructural distribution of immunogold-labeled BAG-75 in the primary spongiosa underlying the rat growth plate is distinct from that for other acidic phosphoproteins, osteopontin and bone sialoprotein. We conclude that BAG-75 self-associates in vitro and in vivo into microfibrillar complexes which are specifically recognized by monoclonal antibody HTP IV-#1. This propensity to self-associate into macromolecular complexes is not shared with acidic phosphoproteins osteopontin and bone sialoprotein. We hypothesize that an extracellular electronegative network of macromolecular BAG-75 complexes could serve an organizational role in forming bone or as a barrier restricting local diffusion of phosphate ions. J. Cell. Biochem. 64:547–564.

Key words: bone acidic glycoprotein-75; self-association; aggregation-dependent neoepitope; macromolecular complexes in vivo and in vitro; sequestration of phosphate ions

Cells of bone and teeth share the unique phenotypic property to produce a mineralized tissue. During bone formation, osteoblastic cells secrete a collagenous matrix which is subsequently mineralized [Baron, 1993]. Microcrystalline carbonated apatite (dahllite) is the predominant mineral phase of bone [Weiner and Traub, 1992]. In addition to type I collagen, bone matrix also contains acidic proteins and phosphoproteins, including osteopontin (OPN),

Abbreviations used: BAG-75, bone acidic glycoprotein-75; BSP, bone sialoprotein (also designated as SP-II); Buffer A, 0.01 M Tris-HCl (pH 7.5), containing 10 mM calcium chloride and 0.15 M sodium chloride; ELISA, enzyme-linked immunosorbent assay; G, 4 M guanidine HCl containing protease and phosphatase inhibitor mixture; G/E, 4 M guanidine HCl/0.5 M EDTA containing protease and phosphatase inhibitor mixture; OPN, osteopontin; TEM, transmission electron microscopy; STEM, scanning transmission electron microscopy.

Contract grant sponsor: NIH, contract grant numbers AR37078, AR40923; Contract grant sponsors: Scientific Education Partnership, Orthopedic Research and Education Foundation, UMKC faculty research grant, NIH biomedical support grant, American Society for Biochemistry and Molecular Biology, Medical Research Council of Canada, FRSQ of Quebec.

*Correspondence to: Jeffrey P. Gorski, Division of Molecular Biology and Biochemistry, School of Biological Sciences, University of Missouri–KC, 5100 Rockhill Road, Kansas City, MO 64110.

Received 3 July 1996; Accepted 23 September 1996

osteonectin, bone sialoprotein (BSP), matrix Gla protein, osteocalcin, decorin, biglycan, and bone acidic glycoprotein-75 (BAG-75) [reviewed in Heinegard and Oldberg, 1989]. The sequences of OPN [Zhang et al., 1990] and BSP [Oldberg et al., 1988a; Fisher et al., 1990] contain Arg-Gly-Asp cell adhesion sites capable of mediating cell adhesion of osteoblastic and osteoclastic cells [Gotoh et al., 1990; Oldberg et al., 1986, 1988b; Somerman et al., 1988; Helfrich et al., 1992; Ross et al., 1993]. Unusual polyacidic amino acid sequences within OPN, BSP, and BAG-75 exhibit a strong species conservation and have been suggested to participate in calcium binding [Gorski, 1992; Boskey et al., 1993; Hunter et al., 1994; Hunter and Goldberg, 1994]. Given the restricted distribution of BSP and BAG-75 to calcified tissues, their elevated calcium binding capacities [Chen et al., 1992], and a strict correlation of acidic macromolecules with cell-controlled mineralization [Lowenstam and Weiner, 1989], it has been suggested that they singly, or together, participate in the nucleation and growth of apatite crystals and in the coupling of formative and resorptive phases in bone turnover [Pinto et al., 1988; Gorski, 1992; Hunter and Goldberg, 1994; Boskey, 1995].

We proposed earlier [Gorski, 1992] that the function of acidic phosphoproteins in bone is dependent upon the formation of specific protein-protein complexes within bone matrix. Ritter et al. [1992] have identified complexes of OPN and osteocalcin using a gel overlay assay. Among noncollagenous bone proteins, BAG-75 alone has been shown to form large self-associated aggregates in vitro [Sato et al., 1992]. Specifically, BAG-75 formed fibrillar structures from monomeric globular subunits ranging in size from 11–132 nm after platinum shadowing. Moreover, competitive binding studies with ^{125}I-BAG-75 and bone particles demonstrated that increasing concentrations of unlabeled BAG-75 brought about a linear increase in binding of the labeled tracer instead of an expected diminution in bound counts [Sato et al., 1992]. These latter results were interpreted as caused by concentration-dependent self-association of BAG-75 on the surface of bone particles. Interestingly, these surface-bound complexes of BAG-75 functioned as a potent inhibitor of osteoclast-mediated bone resorption, whereas soluble OPN, BSP, vitronectin, fibronectin, and thrombospondin were all at least fifty-fold less effective on osteoclasts [Sato et al., 1992]. Findings described here expand upon this initial demonstration of BAG-75 self-association in vitro as well as characterize the specificity of monoclonal antibody HTP IV-#1, which recognizes a neoepitope on BAG-75 complexes. In addition, we demonstrate the formation of macromolecular complexes from ^{3}H-leucine–labeled BAG-75 synthesized by mineralizing explant cultures of bone and growth plate in vitro.

METHODS

Preparation of BAG-75

Calvariae from frozen young adult rat skulls were harvested and processed as described by Gorski et al. [1990]. Contents of pooled fractions containing BAG-75 were dialyzed extensively against 0.5 mM ammonium acetate, stored frozen, and lyophilized prior to use. Concentration of BAG-75 protein was determined by quantitative amino acid analysis.

Preparation and Characterization of Monoclonal Antibody Against BAG-75

B10.S mice were immunized intraperitoneally with purified rat BAG-75 in saline (1–5 µg/injection) every 14 days. After three injections, blood was collected by retroorbital bleeding and the presence of specific antibody tested by enzyme linked immunosorbent assay (ELISA). Mice were boosted with antigen 3 days prior to harvesting of spleens for cell fusions. The protocol used for generation of hybridomas was previously described by Fazekas de St. Groth and Scheidegger [1980]. Briefly, lymphocytes and F/O myeloma cells were mixed at a ratio of 10:1 and centrifuged to form a cell pellet; the cell pellet was resuspended in 50% (v/v) polyethylene glycol 1540 and incubated at 37°C for 90 s. Cells were washed and resuspended in fresh culture medium, and 100 µl aliquots were added to wells of three microtiter plates. Twenty-four hours later, 100 µl of culture medium supplemented with hypoxanthine, aminopterin, and thymidine was added to each well; every 3–4 days thereafter, 100 µl of culture medium was replaced with an equal volume of fresh media containing hypoxanthine, aminopterin, and thymidine, or complete medium successively over a period of about 14 days. When cells reached 75% confluence, culture supernatants were tested for the presence of anti-BAG-75 antibod-

ies. Initial screening was carried out by ELISA using plates coated with either BAG-75, cartilage proteoglycan, human IgG, or bovine serum albumin. Hybridoma HTP IV-#1[1] reacted exclusively with BAG-75 and was cloned in limiting dilution cultures at 1 cell/microtiter well and then recloned at 0.3 cells/well. BALB/c spleen cells served as feeder layer cells in these studies. To prepare ascites fluid, mice were first primed with 0.5 ml of pristane 5 days prior to injection with 1×10^6 hybridoma cells; both injections were made intraperitoneally. Between days 14 and 20, ascites fluid was removed daily for several days. Normal ascites fluid was produced similarly by injection of F/O myeloma cells.

Characterization of MoAb HTP IV-#1 was carried out by Western blotting, ELISA, and immunoprecipitation with crude and purified antigen preparations. Briefly, rat calvariae were extracted with 4 M guanidine–HCl/0.5 M EDTA containing protease and phosphatase inhibitors (G/E), and the entire extract was chromatographed on DEAE-Sephacel as described by Gorski et al. [1990]. A gradient of from 0–2.5 M sodium acetate was used to elute bone matrix proteins; separate aliquots of every tenth fraction were processed for gel electrophoresis and immunoblotting onto cationic nylon membranes, for glycosaminoglycan analyses, or for ELISA [Gorski et al., 1990]. After electroblotting, membranes were incubated for 2 h at room temperature with ascites fluid (1/100) in 50 mM Tris-HCl buffer (pH 7.4), containing 150 mM sodium chloride, 5 mM EDTA, 0.25% gelatin, 0.05% Triton X-100. Next, immunoblots were rinsed with water and incubated for 2 h with horseradish peroxidase conjugated rabbit antimouse IgG (1/200) in 50 mM Tris-HCl buffer (pH 7.4), containing 150 mM sodium chloride, 5 mM EDTA, 0.25% gelatin, and 0.05% Triton X-100. After removal of excess secondary antibody, bound antibody was detected with 4-chloro-1-naphthol in methanol. For ELISA, aliquots of DEAE-column fractions were diluted twofold across rows of microtiter plates into 0.02 M Tris-acetate buffer (pH 7.4), containing 0.01 M EDTA, 0.01 M N-ethyl-maleimide, and 0.005 M phenylmethylsulfonyl fluoride; BAG-75 (1–2 µg/well) served as a positive control. Plates were incubated overnight at 37°C; wells were then rinsed out with 0.02 M Tris-acetate buffer (pH 7.4), containing 0.01 M EDTA, 0.01 M N-ethyl-maleimide, and 0.005 M phenylmethylsulfonyl fluoride, and blocked for 2 h with 1% bovine serum albumin in 0.01 M sodium phosphate buffer (pH 7.4). After being rinsed, wells were incubated for 1 h with ascites fluid (1/3000) in phosphate buffer containing 1% serum albumin. Wells were next rinsed five times with phosphate buffer containing 1.5 mM magnesium chloride, 0.05% Tween 20, 0.5 mM DTT, and 0.05% sodium azide and then incubated with beta-galactosidase–conjugated antimouse IgG antibodies (1/300) for 1 h. Bound enzyme-antibody conjugates were detected with p-nitrophenyl-beta-galactoside (1 mg/ml) in phosphate buffer containing 1.5 mM magnesium chloride and 0.05% sodium azide. Absorbance values were read at 414 nm after raising the pH of assay mixtures above 9.5 with 1 M sodium carbonate.

[1]Definitions: MoAb HTP IV-#1, mouse monoclonal antibody produced by immunization with BAG-75 protein which recognizes BAG-75 antigenic forms in ELISA and immunohistochemistry; anti-BAG-75 antibody (#504), rabbit polyclonal antibody produced by immunization with BAG-75 protein (Mr = 75 kDa) which recognizes BAG-75 antigenic forms in immunoblotting, ELISA, and immunocytochemistry; anti-BAG-75 peptide antibody (#503 or #505), rabbit polyclonal antibody produced by immunization with peptide-albumin conjugate representing N-terminal residues 3–13 which recognizes BAG-75 antigenic forms in immunoprecipitation assays and ELISA.

Immunohistological Methods

Sprague-Dawley rats, either from 1–5 days old or at 6 months of age, were sacrificed by cervical dislocation. Calvariae and tibiae were removed immediately and coated with Tissue-Tek O.C.T. compound (Miles, Inc., Elkhart, IN) prior to cutting 10 µm frozen sections. For immunoperoxidase labeling, frozen sections were incubated with (1/100) anti-BAG-75 peptide antibody (#505) and processed as described by Gorski et al. [1995]; slides were photographed using didynium and neutral density filters. Alternatively, calvarial and tibial tissues were removed, fixed, and decalcified [Magnuson et al., submitted] and resultant sections treated with (1/300) anti-BAG-75 antibody (#504) and with ABC immunodetection kit using biotinylated glucose oxidase and colorimetric substrate (Vector Labs, Inc., Burlingame, CA) before staining for tartrate-resistant acid phosphatase (Sigma Chemical Co., St. Louis, MO). Negative controls consisted of sections treated with preimmune serum.

Micromass cultures of osteoblastic ROS 17/2.8 cells were established following the method of Solursh and Meier [1972]. Day 7 micromass cultures in 35 mm dishes were rinsed free of medium and fixed for 1 h on ice in 2% paraformaldehyde. A drop of OCT compound was then applied to each micromass, the dish immersed in liquid nitrogen, and the cells popped off the dish. Ten micron thick frozen sections were rehydrated in phosphate-buffered saline and incubated for 30 min in normal goat serum diluted 1:5 in phosphate-buffered saline. Sections were rinsed briefly and incubated in (1/80) anti-BAG-75 antibody (#504) for 30 min, rinsed in phosphate-buffered saline, and then incubated for 20 min with (1/300) fluorescein-conjugated IgG fraction of rabbit antimouse IgG (heavy- and light-chain-specific). After washing, sections were next incubated with (1/300) fluorescein-conjugated IgG fraction of goat antirabbit IgG for 20 min prior to rinsing well and mounting in glycerol:phosphate-buffered saline (9:1) containing 1 mg/ml p-phenylenediamine.

Gel Electrophoresis of Immunoprecipitates of Biosynthetically Labeled BAG-75 From Neonatal Explant Cultures of Calvarial and Growth Plate Tissues

Tissues were removed aseptically at 12–36 h after birth from ACI rats. Tibiae from each hind limb were dissected free of soft tissues, and the proximal epiphyses (including the growth plate region and metaphysis) were cut off and sectioned into approximately 2 mm pieces. Tissue segments were maintained briefly in leucine-depleted F-12 media until biosynthetic labeling was begun. Calvariae were removed intact with associated endosteal and periosteal layers and each calvaria cut into 2 mm segments. Calvarial and growth plate explants were then cultured separately for 28 h at 37°C and 5% CO_2 in 6 ml of F-12 media containing ^{3}H-leucine (100 μCi/ml) and 0.1 mM leucine. Cells were killed by three cycles of freeze/thawing. Solid guanidine-HCl and 3-[(3-cholamidopropyl)-dimethylammonio]-1-propanesulfonate were added to each culture flask to a final concentration of 4 M and 0.5%, respectively, and radiolabeled BAG-75 was extracted from explants by mixing for 1 h at 4°C. Following a short centrifugation step to pellet tissue fragments, extracts were removed and dialyzed sequentially against 4 M guanidine-HCl containing protease and phosphatase inhibitors (G) for 24 h and then against two changes of 6 M urea containing inhibitors over the next 48 h [Gorski et al., 1990]. At this stage, SDS, deoxycholate, and Triton X-100 detergents were added to the extract fraction to a final concentration of 0.1% each. Extracts were then dialyzed against 0.1 M Tris-acetate buffer (pH 7.5), containing 10 mM EDTA, 40 mM ϵ-amino-n-caproic acid, 10 mM benzamidine HCl, 0.25 mg/ml phenylmethylsulfonylflouride, 0.1% SDS, 0.1% deoxycholate, 0.1% Triton X-100, and 0.02% sodium azide, and then centrifuged at 100,000*g* for 1 h prior to setting up immunoprecipitations. This extraction and processing protocol was adapted from that of Bumol et al. [1984] and results in solubilization of 90–95% of radiolabeled calvarial and growth plate proteins [Gorski et al., 1990]; 5–10% of labeled proteins were recovered upon subsequent extraction of tissue residues with G/E. Immunoprecipitations followed that described previously [Gorski et al., 1990]; immunoprecipitates were subjected to liquid scintillation counting, gel electrophoresis, and autoradiography.

Phosphate Analysis

Preparations of phosphoproteins were analyzed directly for inorganic phosphate by both the colorimetric and electrochemical methods. Colorimetric analyses followed the method of Bartlett [1959]. Electrochemical analyses were run on an AS 410 ion exchange column with a Dionex ion chromatograph and electrochemical detector (range 30 μS). Ion separation was accomplished with a linear gradient of from 50–200 mM sodium hydroxide; 70 mM sulfuric acid was pumped continuously through the anion micromembrane suppressor. Determinations were made in both methods by reference to a standard curve constructed with a comnmercial phosphate standard.

Colloidal-Gold Immunocytochemistry of BAG-75 In Vivo

For in vivo studies, male Wistar rats ranging from 30–100 g were anesthetized with chloral hydrate and perfused through the heart and into the aorta for approximately 20 s with lactated Ringer's solution. This was followed by perfusion with 1% glutaraldehyde or 4% paraformaldehyde plus 0.1% glutaraldehyde in 0.08 M sodium cacodylate buffer (pH 7.3) containing 0.05% calcium chloride for 15 min. Tibiae were dissected and further fixed by immersion in the

same fixative overnight at 4°C. Samples were decalcified in 4.13% disodium EDTA containing 0.1% glutaraldehyde for 21 days followed by washing with 0.1 M sodium cacodylate buffer (pH 7.3) containing 5% sucrose. Metaphyseal segments of the tibia, including the growth plate, were dehydrated through a graded ethanol series and embedded in LR White acrylic resin that was polymerized at 58°C.

For electron microscopy, thin sections (80–100 nm) of the metaphysis were cut with a diamond knife on a Reichert Ultracut E microtome (Leica, Inc., Deerfield, IL) and processed for immunocytochemistry. The protein A-gold immunocytochemical technique [reviewed by Bendayan, 1989] was applied to thin sections of the samples as described previously [McKee et al., 1990]. Briefly, grid-mounted tissue sections were floated for 5 min on a drop of 0.01 M phosphate-buffered saline (PBS) containing 1% ovalbumin and then transferred and incubated for 1 h at room temperature on a drop of rabbit anti-BAG-75 antibody (#504). Sections were then rinsed with PBS and placed again on PBS–1% ovalbumin for 5 min, followed by incubation for 30 min at room temperature with protein A-gold complex (gold particles of approximately 14 nm in diameter). Tissue sections were then washed thoroughly with PBS, rinsed with distilled water, and conventionally stained with uranyl acetate and lead citrate prior to examination by transmission electron microscopy (TEM) using a JEOL JEM 2000 FX-II instrument (JEOL USA, Inc., Peabody, MA) operated at 80 kV.

STEM and X-Ray Microanalysis of BAG-75 Aggregates Formed In Vitro

BAG-75 preparations were lyophilized to dryness and rehydrated at a concentration of 96.5 nM in 50 mM Tris-acetate buffer (pH 7.5), containing 150 mM sodium chloride, 1 mM calcium chloride and 0.02% sodium azide. Aggregates were deposited onto electron microscope grids as described above, stained briefly with uranyl acetate, and examined by TEM. Electron probe X-ray microanalysis was performed on BAG-75 aggregates in the scanning transmission electron microscopy (STEM) mode of a JEOL 2000 FX-II electron microscope operating at 200 kV and equipped with an energy-dispersive X-ray detector system (Link eXL-II; Oxford Instruments, Bucks, UK). X-rays were recorded using 100 s of counting time, and analyzed areas corresponded approximately to a single macromolecular complex.

Light Scattering Measurements

Scattering measurements were performed at 350 nm at a scattering angle of 90° at 25°C using an Aminco Bowman Series 2 Luminescence spectrophotometer (SML Instruments, Inc., Urbana, IL). Buffers were filtered through a 0.2 µm membrane before use. Preparations of BAG-75 were lyophilized to dryness and rehydrated with 0.05 M Tris-HCl buffer (pH 7.4) containing 0.15 M sodium chloride and 0.02% sodium azide. BAG-75 was diluted two- to 4,096-fold into siliconized tubes with the same buffer; an equal volume of buffer containing 0, 2, 10, or 20 mM calcium chloride was then added to all samples. Measurements were made after a 20–24 h incubation period at 37°C.

RESULTS

BAG-75 Is Localized to Areas of New Bone Formation in Calvaria and Growth Plate

Figure 1A depicts the immunohistochemical distribution of BAG-75 antigenicity within neonatal calvarial bone. A tangential view of an undecalcified calvarial section demonstrates that BAG-75 is localized specifically to areas undergoing osteogenesis and is not found in surrounding soft, undifferentiated mesenchymal tissue or in the overlying epithelium and associated hair follicles (Fig. 1A). Use of preimmune rabbit serum gave only background staining (Fig. 1B). The immunologic distribution of BAG-75 in young adult tibial metaphyseal bone appears to reflect its specific biosynthesis and secretion by osteoblasts. In particular, BAG-75 antigen was restricted to spherical matrix domains surrounding individual osteoblasts in the primary and secondary spongiosa regions (Fig. 1C). Matrix representing the residual calcified cartilage core was negative. Based on metaphyseal morphology (Jee, 1983), the limits of BAG-75 immunostaining appear to coincide with the interface between new woven bone and the older calcified cartilage matrix.

Monoclonal HTP IV-#1 Recognizes Macromolecular Complexes of BAG-75 In Vitro and In Vivo

Monoclonal antibody HTP IV-#1 was produced by injection of aggregated BAG-75 and exhibits a specificity for complexes of BAG-75.

This specificity was demonstrated in several ways. First, MoAb HTP IV-#1 recognizes purified BAG-75 adsorbed to microtiter wells as indicated by the titration in Table IA. Immunoreactivity was detected out to a dilution of greater than 62,500, while the normal ascites fluid control was largely without effect, which supports a requirement for immunoglobulin. Control studies with rat osteopontin, bone sialoprotein, decorin, biglycan, and bovine cartilage proteoglycan were also negative (not shown). The specificity of MoAb HTP IV-#1 for complexes of BAG-75 is demonstrated by results of the competition experiment shown in Table IB. MoAb HTP IV-#1 (1:1000) was preincubated with different concentrations of BAG-75 in the presence of serum albumin for 1.5 h at 37°C. Antibody-antigen mixtures were then added separately to microtiter wells which had been previously coated with 5 µg BAG-75, washed, and blocked with albumin to cover up excess binding sites. After 30 min, free antibody was washed out, and bound antibody was determined colorimetrically. Instead of an expected >90% reduction consistent with a twenty-fold excess of soluble vs. adsorbed BAG-75, preincubation with 1.2–10 µg of BAG-75 increased binding of MoAb HTP IV-#1 by up to 44% compared to controls (Table IB). Other testing has shown that MoAb HTP IV-#1 also does not recognize soluble BAG-75 antigenic forms in radioimmunoassays (not shown). These findings indicate BAG-75 in solution self-associates with BAG-75 adsorbed microtiter wells, resulting in greater reactivity with MoAb HTP IV-#1 compared to controls. Second, a specificity of MoAb HTP IV-#1 for surface-bound or macromolecular complexes of BAG-75 is supported by immunoblotting studies with fractions from an ion-exchange separation of a total G/E extract of calvariae. In this way, immunoreactivity could be correlated with known elution profiles of

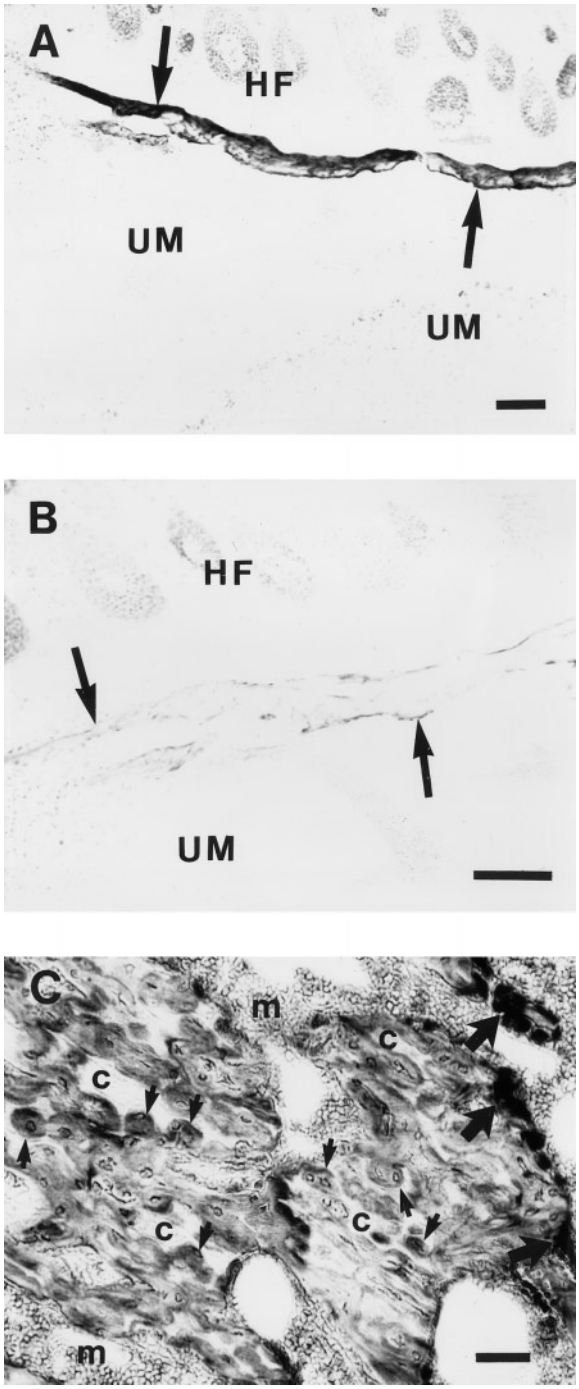

Fig. 1. Immunohistological localization of bone acidic glycoprotein-75 in neonatal calvarial and young adult growth plate tissues. **A:** Tangential view of 5-day-old undecalcified rat calvarial tissue demonstrates that BAG-75 is restricted to areas of new bone formation. BAG-75 antigen was visualized in undecalcified section with anti-BAG-75 antipeptide antibody (#505) via immunoperoxidase detection system and diaminobenzidine stain as described in Methods; slides were counterstained with hematoxylin. Mineralized neonatal calvarial bone matrix and osteoblasts (*arrows*) stain positively for BAG-75, whereas hair follicles (HF) and undifferentiated mesenchyme (UM) away from the mineralized matrix are negative. Bar = 100 µm. **B:** Negative neonatal calvarial control. Preimmune rabbit serum was substituted for the primary antibody and processed as described above. Mineralized neonatal calvarial bone matrix and osteoblasts are indicated (*arrows*). Bar = 100 µm. **C:** In young adult rat growth plate, BAG-75 is restricted to areas of matrix deposited by osteoblasts within the primary and secondary spongiosa. BAG-75 antigenicity was localized in this decalcified section to spherical matrix domains surrounding individual or pairs of osteoblasts (*small arrows*) with anti-BAG-75 antibody (#504) and glucose oxidase detection system (see Methods). Osteoclasts were identified by staining for tartrate-resistant acid phosphatase (*large arrows*). c, residual calcified cartilage core; m, unstained bone marrow cells. Bar = 50 µm.

TABLE I. Immunodetection of Complexes of BAG-75 with MoAb HTP IV-#1

A: Titration of MoAb HTP IV-#1 with surface-bound BAG-75[a]

Dilution	MoAb HTP IV-#1 (O.D. 400 nm)	Normal ascites fluid (O.D. 400 nm)
1/100	1.247	0.091
1/500	0.802	0.037
1/2500	0.450	0.019
1/12,500	0.165	0.020
1/62,500	0.049	0.014
1/312,500	0.028	0.016

B: Soluble BAG-75 does not compete with but rather increases binding of MoAb HTP IV-#1 to adsorbed BAG-75 in competitive ELISA[b]

Concentration of soluble competitor BAG-75 (µg/ml)	O.D. 400 nm (percent of control)
10	144
5	119
2.5	109
1.2	115
0.6	102

[a]All microtiter wells were incubated with an input concentration of 5 µg/ml BAG-75 and then washed, resulting in retention of approximately 0.5 µg antigen/well.

[b]Soluble BAG-75 was incubated with MoAb HTP IV-#1 (1/1,000) for 1.5 h at 37°C prior to addition of the mixture to microtiter wells containing adsorbed BAG-75 and development of colorimetric reaction. All microtiter wells were initially incubated with an input concentration of 5 µg/ml BAG-75 and then washed, resulting in retention of approximately 0.5 µg antigen/well; wells were blocked with an excess of serum albumin before exposure to MoAb HTP IV-#1 with or without soluble BAG-75.

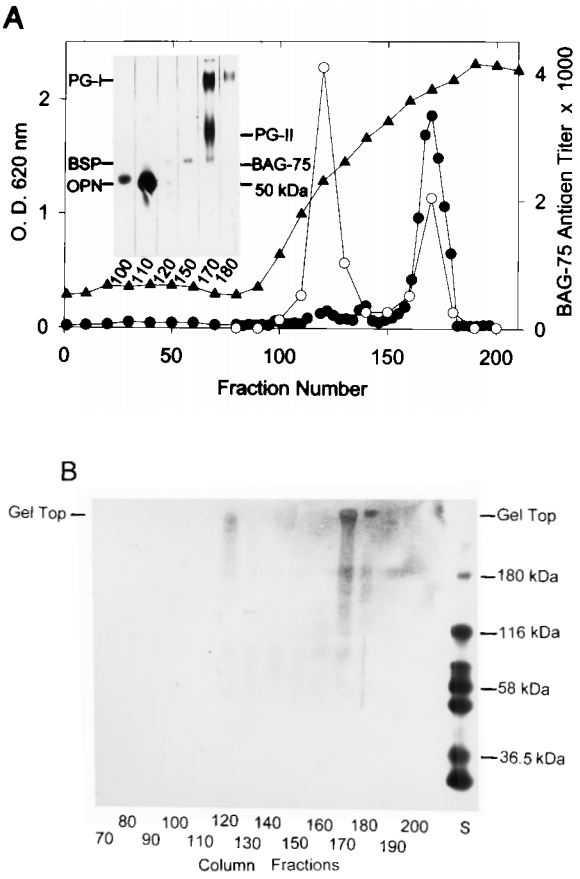

Fig. 2. Monoclonal antibody HTP IV-#1 exhibits a specificity for complexed forms of BAG-75. **A:** Fractions resulting from chromatography of total G/E extract of rat calvariae on DEAE-Sephacel were analyzed by ELISA and for glycosoaminoglycan chain content as described in Methods. **Inset:** Gel pattern after Stains-All staining of selected fractions. ●, O.D. 620 nm; ○, BAG-75 antigen titer. A salt gradient from 0 to 2.5 M sodium acetate is depicted by a plot of conductivity measurements (▲). **B:** Western blot of fractions from ion-exchange separation of total G/E extract. Individual fractions depicted in Fig. 2A were subjected to gel electrophoresis and transfer onto cationic nylon membrane as described in Methods. Binding of MoAb HTP IV-#1 to the resultant blot was detected colorimetrically with horseradish peroxidase–conjugated secondary antibodies. Two regions of immunoreactivity appear as smears in fractions 120 and 170 extending from the top of the running gel to the 100 kDa molecular weight range. Migration positions of standards are shown on the figure. S, prestained globular protein standards.

individual bone matrix proteins. Based on gel electrophoretic banding patterns (Fig. 2A, inset) and glycosaminoglycan contents of fractions (Fig. 2A), OPN, BAG-75 Mr = 50 kDa fragment[2], BSP, BAG-75, and decorin/biglycan were detected in fractions 100–110, 120, 120–150, 150–180, and 170–180, respectively. ELISA analysis with MoAb HTP IV-#1 demonstrated two peaks of immunoreactivity in fractions 120 and 170 (Fig. 2A), regions enriched with BAG-75 Mr = 50 kDa fragment and BAG-75 [Gorski et al., 1990], respectively. Background levels of immunoreactivity were observed with fractions enriched in other bone matrix components. Immunoreactivity on Western blots corresponded to the same peak fractions (Fig. 2B). The immunoblots documented specific recognition of high molecular weight complexes of BAG-75; immune staining in lanes 120 and 170 appeared as a smear extending from the top of the running gel down to the 100,000 kDa molecular weight range (Fig. 2B). This pattern is very similar to that for aggregate forms produced from purified monomeric BAG-75 which migrated both at the top of the running gel and as a broad band between Mr = 120,000 and

[2]N-terminal sequencing of Mr = 50 kDa fragment purified from bone yielded the same N-terminus as BAG-75 [J.P. Gorski and C. Fullenkamp, unpublished results].

180,000 [Gorski et al., in press]. Relative reactivities of the two peaks of immunogenicity were somewhat different in ELISA and immunoblotting assays; these differences may be due to competition of distinct populations of contaminating proteins with BAG-75 forms for adsorption to microtiter wells. Efforts to increase the intensity of the staining reaction on Western blots were restricted by the low transfer efficiency of the large complexes. MoAb HTP IV-#1 displayed only minor reactivity with the monomeric 50 kDa fragment or BAG-75 which are present in fractions 110–130 and 150–180, respectively (Fig. 2B); these latter forms are readily detected with either anti-BAG-75 peptide (#503 or #505) or anti-BAG-75 (#504) antibodies [Gorski et al., 1990]. Taken together, results in Table I and Figure 2 indicate the MoAb HTP IV-#1 preferentially binds to a neoepitope on macromolecular complexes of BAG-75.

It was of interest to determine whether MoAb HTP IV-#1 would detect BAG-75 in rat tissues or micromass cultures of osteoblastic ROS 17/2.8 cells. As illustrated in Figure 3A, discrete, punctate patches of intense immunoreactivity were observed in the primary spongiosa underlying the tibial growth plate. Mineralized regions of the primary spongiosa appear as irregular bleached areas under phase contrast due to their differential refractive properties. No staining for BAG-75 was observed in cartilagenous zones of the growth plate with either MoAb HTP IV-#1 (Fig. 3A) or anti-BAG-75 protein antibodies (#504) (not shown). Micromass cultures of osteoblastic cells, which establish an extracellular matrix compartment, also reacted positively with MoAb HTP IV-#1 (Fig. 3B). Immunofluorescent staining was predominantly focal and punctate in appearance and seemed to represent antigen near cell membranes or within a territorial matrix. Diffuse, low level staining was also observed throughout the cell mass. Cultures treated with normal ascites fluid were negative (Fig. 3C). These results show that MoAb HTP IV-#1 detects a focal distribution of BAG-75 complexes in bone which are restricted to mineralized areas in the primary spongiosa.

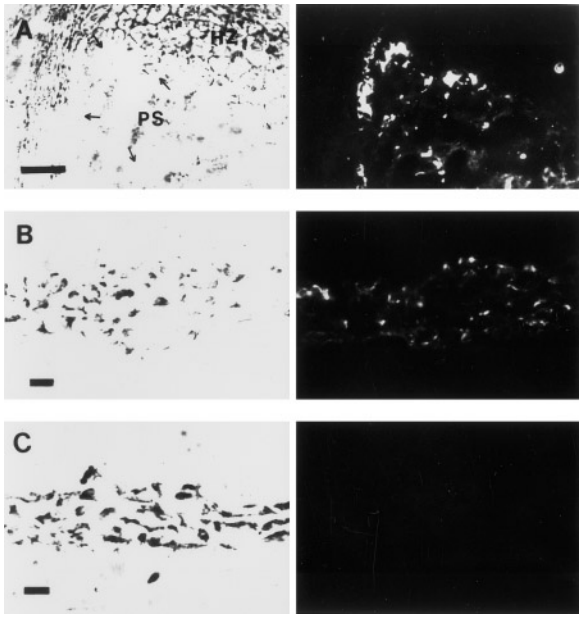

Fig. 3. Immunohistochemical identification of complexed BAG-75 antigen antigen in rat growth plate and micromass cultures of osteosarcoma cells with MoAb HTP IV-#1. **A:** Day 3 neonatal growth plate. Frozen sections were processed for immunofluorescence microscopy as described in Methods. Selected areas of immunoreactivity which correspond with mineralized areas visualized under phase contrast are marked (*arrows*). Phase contrast (**left**) and fluorescence (**right**) images of the same section are shown. HZ, hypertrophic zone; PS, primary spongiosa. Bar = 100 μm. **B:** Day 7 micromass culture of ROS 17/2.8 cells. See Methods for protocol. Phase contrast (**left**) and fluorescence (**right**) images of the same section incubated with MoAb HTP IV-#1 are shown (staining seen in the center of the micromass appears to be stronger than at its edges). Bar = 100 μm. **C:** Negative control. Micromass culture treated with spent F/O myeloma culture media. Phase contrast (**left**) and fluorescence (**right**) images of the same section are shown. Bar = 10 μm.

BAG-75 Synthesized by Neonatal Bone Explants Is Incorporated Into Large Macromolecular Complexes

Immunoprecipitation of biosynthetically labeled BAG-75 from monolayer cultures of rat calvarial cells and from ROS 17/2.8 cells with antipeptide antibody (#503) yields two antigenic forms, monomeric BAG-75 and a fragment at Mr = 50 kDa [Gorski et al., 1990]. In contrast, similar immunoprecipitates from 28 h cultures of neonatal calvarial and growth plate tissues were composed of complexed BAG-75 forms greater than Mr = 200 kDa (Fig. 4) Confirming results with MoAb HTP IV-#1, a band at the top of the running gel and a doublet band near Mr = 200 kDa were specifically immunoprecipitated from calvarial explants (Fig. 4, lane 1 vs. lane 3) using a second anti-BAG-75 antibody (#505). In controls, calvarial immunoprecipitates contained an expected OPN band at Mr = 50 kDA, along with a fragment band observed previously [Zhang et al., 1990] (Fig. 4, lane 2); similar bands were observable in growth plate samples with longer exposure of autoradio-

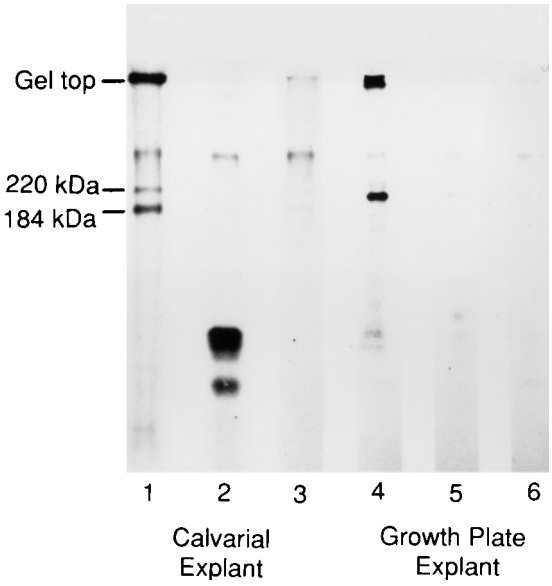

Fig. 4. Gel electrophoresis of immunoprecipitates of biosynthetically labeled BAG-75 and OPN from explant cultures of neonatal calvaria and growth plate. Extracts of ^{3}H-leucine–labeled calvarial and tibial growth plate explant cultures were immunoprecipitated with anti-BAG-75 peptide antibody (#503), monoclonal anti-OPN antibodies, or preimmune serum as described in Methods. Immunoprecipitates were solubilized and electrophoresed on 7.5% denaturing gels under reducing conditions. Calvarial samples were run in *lanes 1–3* and growth plate samples in lanes *4–6.* Lanes 1, 4: Anti-BAG-75 peptide antibody (#503). Lanes 2, 5: Anti-OPN antibodies. Lanes 3, 6: Preimmune rabbit serum.

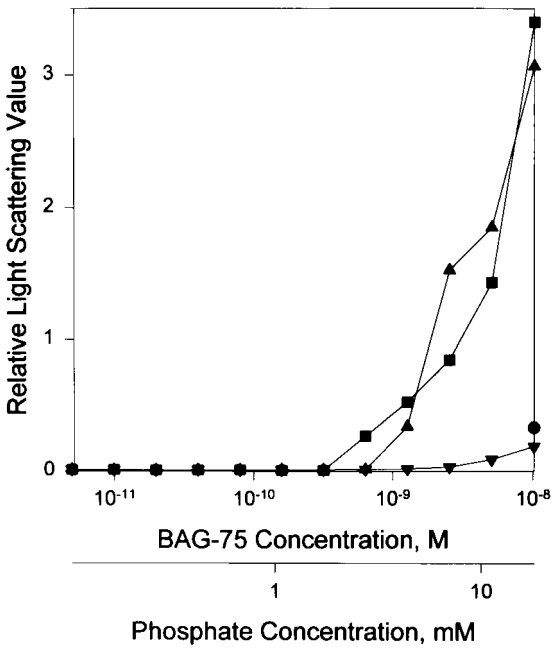

Fig. 5. Light-scattering analysis of BAG-75 preparation in the presence of 0–10 mM calcium chloride. BAG-75 was lyophilized and rehydrated at a concentration of 2.04×10^{-8} M in the presence of 0.05 M Tris-HCl buffer (pH 7.5) containing 0.15 M sodium chloride; aliquots of BAG-75 were then diluted in sequential twofold steps with buffer containing either 2, 10, or 20 mM calcium chloride. After a 20–24 h incubation period at 37°C, samples were analyzed by light-scattering measurements using a spectrofluorometer with emission and excitation wavelengths of 350 nm. Light-scattering values are plotted on a relative scale vs. the concentration of BAG-75. For clarity, light-scattering values are also plotted vs. the concentration of inorganic phosphate in the BAG-75 preparation. Results shown are representative of that obtained with three separate preparations. ■, 10 mM calcium; ▲, 5 mM calcium, ▼, 1 mM calcium; ●, no added calcium.

graphs (data not shown). It should be emphasized that our protocol routinely extracts >90–95% of radiolabeled proteins from explants into a 100,000*g* supernatant fraction. All newly synthesized (and labeled) BAG-75 extracted from these explants was present within aggregates. We hypothesize that this may reflect the functional state of cells on the surface of explants accessible to the ^{3}H-leucine precursor. Monomeric BAG-75 Mr = 50 kDa fragment and BAG-75 (Mr = 75 kDa), as well as similar sized aggregated forms, were detected in immunoblots of G/E extracts of calvaria and growth plate tissues with this same antibody [Gorski et al., 1990].

Macromolecular Complexes of Purified BAG-75 Sequester Phosphate Ions

To examine the effect of calcium ion concentration on self-association, BAG-75 was incubated over a range of concentrations (10^{-8} to 10^{-12} M) in 0.05 M Tris-acetate buffer (pH 7.5), containing 0.15 M sodium chloride, and 0, 1, 5 or 10 mM calcium chloride. As shown by light scattering results in Figure 5, particulate complexes were formed in the presence of 5 and 10 mM calcium. Visual inspection confirmed the presence of particulate complexes in these samples. In contrast, no particulate matter was evident in BAG-75 samples with 1 mM calcium or without added calcium since light-scattering values for these two conditions were comparable and near background levels (Fig. 5).

Although the results in Figure 5 were initially interpreted as being due to calcium-induced formation of BAG-75 protein-protein complexes, electron microscopic analyses, X-ray microanalyses, and X-ray diffraction results demonstrated that the majority of the observed light-scattering signal was due to the formation of inorganic crystals of calcium phosphate. Specifically, particles formed with BAG-75 (5.7×10^{-7} M) in the presence of 10 mM calcium chloride were composed of loose

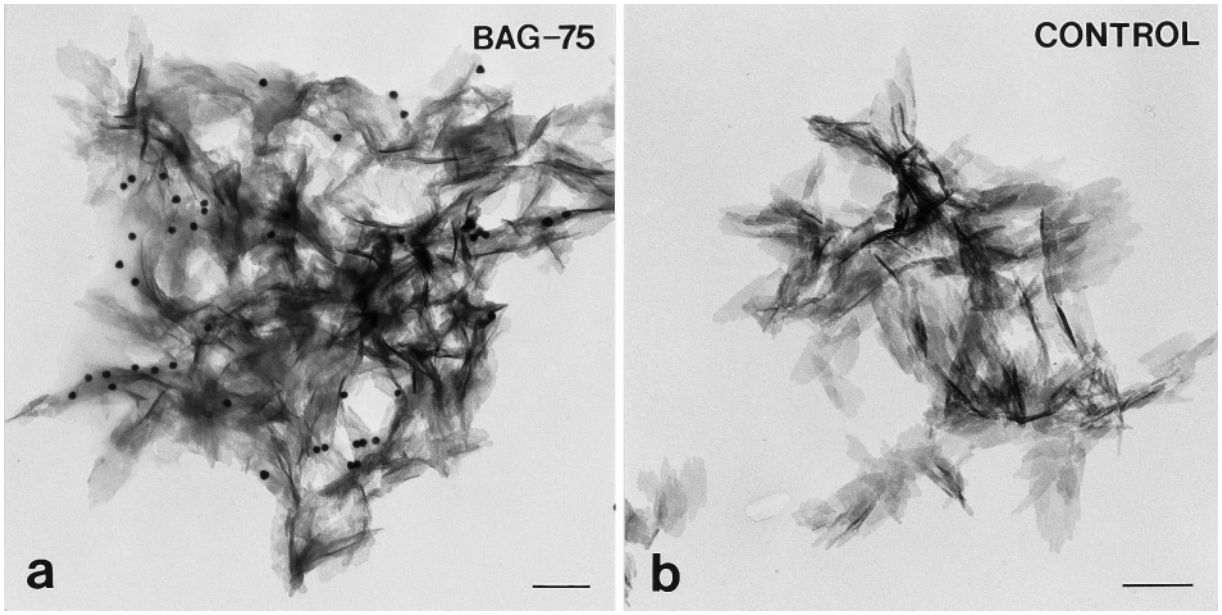

Fig. 6. Immunoelectron microscopic analysis of hydroxyapatite crystals formed by bone acidic glycoprotein-75 preparations in the presence of 10 mM calcium chloride. **a:** BAG-75 associated with hydroxyapatite crystals formed in vitro is recognized by anti-BAG-75 (#504) antibodies. Specific antibody-dependent gold-particle labeling for BAG-75 is associated with thin, plate-like crystallites of hydroxyapatite. Bar = 0.1 µm. **b:** Negative immune control. Hydroxyapatite crystals formed in vitro with BAG-75 were incubated with an unrelated, antiamelogenin antibody (courtesy of Dr. A. Nanci). Bar = 0.1 µm.

composites of very thin inorganic crystallites with lengths ranging between 50 and 100 nm in this specimen (Fig. 6A). BAG-75 antigen was bound to the calcium crystals as evidenced by immunolabeling with anti-BAG-75 antibody (#504) and gold particles. Control incubations with an unrelated antibody or protein A-gold alone (not shown) confirmed the specificity of the former immunoreaction (Fig. 6B). Subsequently, powder X-ray diffraction analyses [Gorski, Kremer, and Johns, unpublished results] on crystals formed with BAG-75 and 5 mM calcium chloride identified them as a poorly crystalline form of hydroxyapatite, $Ca_5(PO_4)_3OH$. Formation of hydroxyapatite upon addition of 5–10 mM calcium chloride to preparations of BAG-75 prompted a search for the source of phosphate in these preparations. Millimolar concentrations of phosphate were found to be a consistent component of five separate preparations of BAG-75 (Table II). Both colorimetric and ion chromatographic electrochemical detection methods for inorganic phosphate yielded similar findings. The concentration of phosphate in BAG-75 preparations ranged between 0.8 and 2.5 mM (Table II); however, calcium ion concentrations were at or below the limit of detection (25.0 µM) for atomic absorption spectrophotometry. For reference, the concentration of phosphate in BAG-75 samples was also plotted vs. light-scattering values in Figure 5. Hydroxyapatite crystallization was first observed at 2.25 and 1.12 mM phosphate in the presence of 5 and 10 mM calcium, respectively (Fig. 5), concentrations of these ions able to form hydroxyapatite crystals in the absence of BAG-75. We reason that the most likely source of contamination is from the potassium phosphate used to elute BAG-75 from hydroxyapatite during the last step of its purification [Gorski and Shimizu, 1988]. However, since purified BAG-75 preparations are dialyzed extensively before use, the concentrations of phosphate present are at least

TABLE II. Phosphate and Calcium Ion Contents of BAG-75 Preparations

Preparation	Protein (nM)	Phosphate (mM)	Calcium[a] (µM)
10	7.14	1.44	—
11	8.06	2.49	32.4
12	9.70	1.00	47.4
13	17.8	0.81	—
14	5.08	0.93	—
14	5.08	1.03[b]	—

[a]Determined by atomic absorption spectrophotometry; dashes represent values below the limit of detection (24.7 µM).

[b]Phosphate analysis for preparation 14 was repeated on ion chromatograph with electrochemical detection.

1,000-fold higher than predicted from simple exchange calculations. Phosphate analyses on final dialyzate volumes found values near 0.05 mM, an indication that phosphate ions associated with BAG-75 were not freely exchanging with those in the larger solution phase. Since the quantity of phosphate present represents a 45,000–300,000-fold molar excess over that for BAG-75 (Table II), this amount of phosphate cannot be due entirely to direct binding to BAG-75. Microscopic surveys of BAG-75 preparations found no evidence for a crystalline phase. Thus, we hypothesize that BAG-75 self-associates to form complexes on the inner surface of dialysis membranes early in the exchange process; surface-bound, electronegative, BAG-75 complexes would constitute a charged barrier inhibiting exchange of (potassium) phosphate ions. According to this rationale, formation of hydroxyapatite crystals after addition of calcium is an indirect consequence of the propensity of BAG-75 to sequester millimolar concentrations of phosphate ion.

Morphological analysis of BAG-75 preparations reconstituted in 1 mM calcium chloride confirmed the existence of unique macromolecular, self-associated complexes of BAG-75 (Fig. 7); similar results were obtained with BAG-75 in the absence of calcium (data not shown). As observed by light microscopy, hydrated BAG-75 complexes are roughly spherical in shape and range from 20–35 μm in diameter. Complexes appear to be composed of a collapsed latticework of crisscrossing fibrils. In some cases, individual complexes (Fig. 7A,B, arrow) exhibited thin "tails" of up to 27 μm in length. Dense particles were also associated with each macromolecular complex of BAG-75 (Fig. 7A–C, arrowheads). Buffer controls without BAG-75 (not shown) were devoid of comparable structures. A search for inorganic hydroxyapatite crystals proved negative, as indicated by a lack of diffraction of polarized light and by an absence of

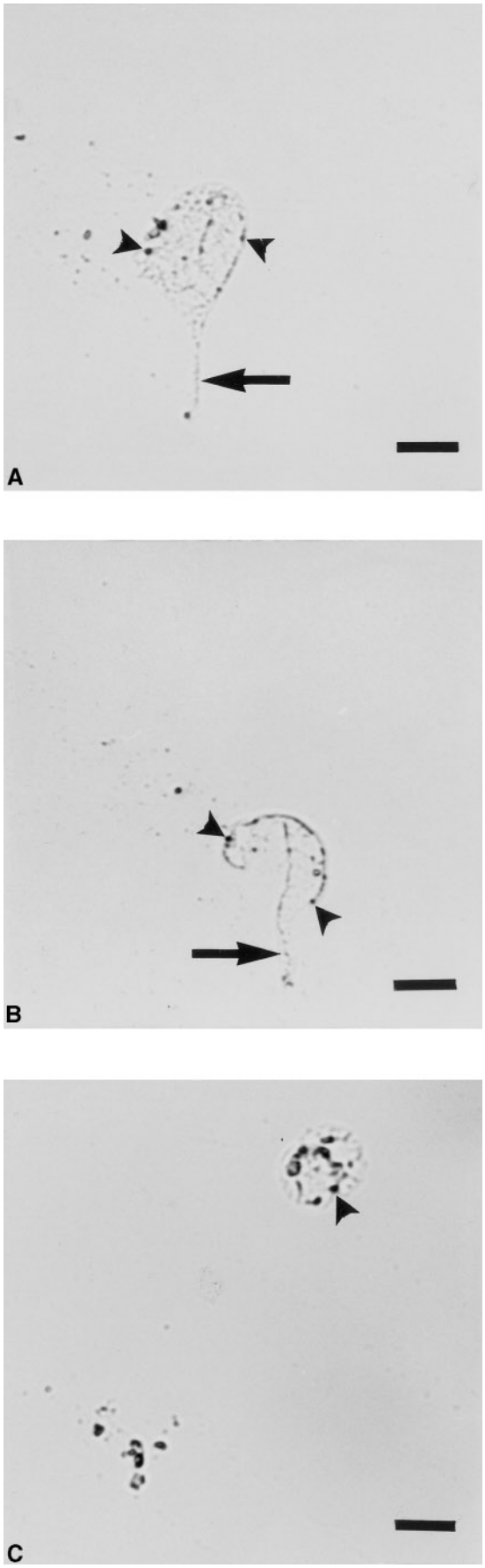

Fig. 7. Light microscopic identification of macromolecular complexes of BAG-75. **A–C:** Representative composite views of macromolecular complexes formed by purified BAG-75. BAG-75 was lyophilized to dryness and rehydrated at a concentration of 96.5 nM in 50 mM Tris-acetate buffer (pH 7.5) containing 150 mM sodium chloride, 1 mM calcium chloride, and 0.02% sodium azide. Droplets containing BAG-75 complexes were placed on a glass slide, coverslipped, and photographed with a differential interference contrast objective. Individual complexes occasionally exhibited thin "tails" of up to 27 μm in length (*arrow,* A, B). Dense particles were also associated with macromolecular complexes of BAG-75 (*arrowheads*). Bar = 20 μm.

crystalline material as assessed by TEM (see Fig. 8a).

Ultrastructural and elemental analyses were performed on macromolecular BAG-75 complexes to examine their morphology in greater detail, to confirm their proteinaceous nature, and to analyze for associated calcium and phosphorus atoms. Dehydrated BAG-75 complexes viewed by STEM were also spherical in shape, although smaller in overall dimensions (4–9 μm in diameter) (Fig. 8A, inset) than aqueous structures observed by light microscopy (Fig. 7). At low magnification, complexes contained numerous small folds and overlapping regions which gave the impression of a collapsed structure that may have been more expanded under aqueous conditions. Higher magnification TEM imaging of the periphery of individual BAG-75 complexes, where specimen thickness and overlap of organic material were minimal, revealed an extensive network of fine fibrils (Fig. 8A).Thin fibrils, approximately 10 nm in diameter and capable of up to 70–80° bends, formed a fringe that often extended away from the main body of complexes by as much as 500 nm. Individual fibrils sometimes joined together to form larger composite strands (Fig. 8A). When X-ray microanalysis was carried out, calcium and phosphorus were enriched in all macromolecular BAG-75 complexes examined (Fig. 8B). These elements were not detected in background spectra from adjacent areas of supporting film alone (data not shown). Peaks for Ni and U are derived from the electron microscope grid and the heavy-metal contrasting agent, respectively (Fig. 8B). The ratio of phosphorus to calcium signals for individual complexes was relatively constant (1.25 ± 0.11); however, the size of these peaks differed by fourfold among BAG-75 complexes sampled.

Ultrastructural Distribution of BAG-75 Within the Primary Spongiosa Underlying the Tibial Growth Plate

The distribution of BAG-75 antigenicity in the tibial metaphysis (including growth plate) was determined with anti-BAG-75 protein antibody (#504) and protein A-gold (Fig. 9). Intense immunolabeling was observed throughout the mineralized bone matrix of the primary spongiosa. This labeling pattern did not include regions of unmineralized osteoid and the calcified cartilage of the growth plate, although some gold particles occasionally were present over the cement line at the bone-calcified cartilage interface. MoAb HTP IV-#1 did not recognize BAG-75 antigen in tissues processed for immunoelectron microscopy. Unlike the "patchy" distribution of labeling routinely observed for noncollagenous proteins OPN, osteocalcin, α_2-HS-glycoprotein, and BSP [reviewed in McKee and Nanci, 1993], BAG-75 labeling was distributed more diffusely throughout the mineralized bone matrix compartment, although gold particles often gave the impression of being more discretely and irregularly arranged in somewhat linear patterns, roughly circumscribing regions of unlabeled matrix (Fig. 9).

DISCUSSION

Results presented here support the following new conclusions. First, MoAb HTP IV-#1 specifically recognizes a neoepitope on complexes of BAG-75 or a Mr = 50,000 fragment. Second, BAG-75 complexes exist in situ as evidenced by immunofluorescent staining of frozen sections of neonatal tibial metaphysis and micromass cultures of osteosarcoma cells with MoAb HTP IV-#1. Third, radiolabeled BAG-75 was shown to be incorporated into macromolecular complexes within 28 h after synthesis by newborn calvaria. BAG-75 complexes were immunoprecipitated from bone explant cultures with a second anti-BAG-75 antibody (#503), while similar immunoprecipitates from monolayer cultures of osteoblastic cells [Gorski et al., 1990] contained only monomeric Mr = 75 kDa BAG-75 and a Mr = 50 kDa fragment. Fourth, purified BAG-75 self-associates in vitro to form spherical structures composed of a fine fibrillar meshwork. These complexes have the capacity to sequester large amounts of phosphate ions as evidenced by x-ray microanalysis of BAG-75 complexes and because purified preparations of BAG-75 contain millimolar concentrations of phosphate, even after extensive dialysis. Fifth, the ultrastructural distribution of immunogold-labeled BAG-75 in the primary spongiosa of the tibial metaphysis is distinct from that of acidic phosphoproteins OPN and BSP. Based upon these data, we conclude that BAG-75 self-associates in vitro and in vivo into microfibrillar complexes which are recognized by monoclonal antibody HTP IV-#1. We hypothesize that macromolecular complexes of BAG-75 may function as extracellular electronegative barriers restricting local diffusion of phosphorus ions, thereby facilitating nucleation of apatite in bone.

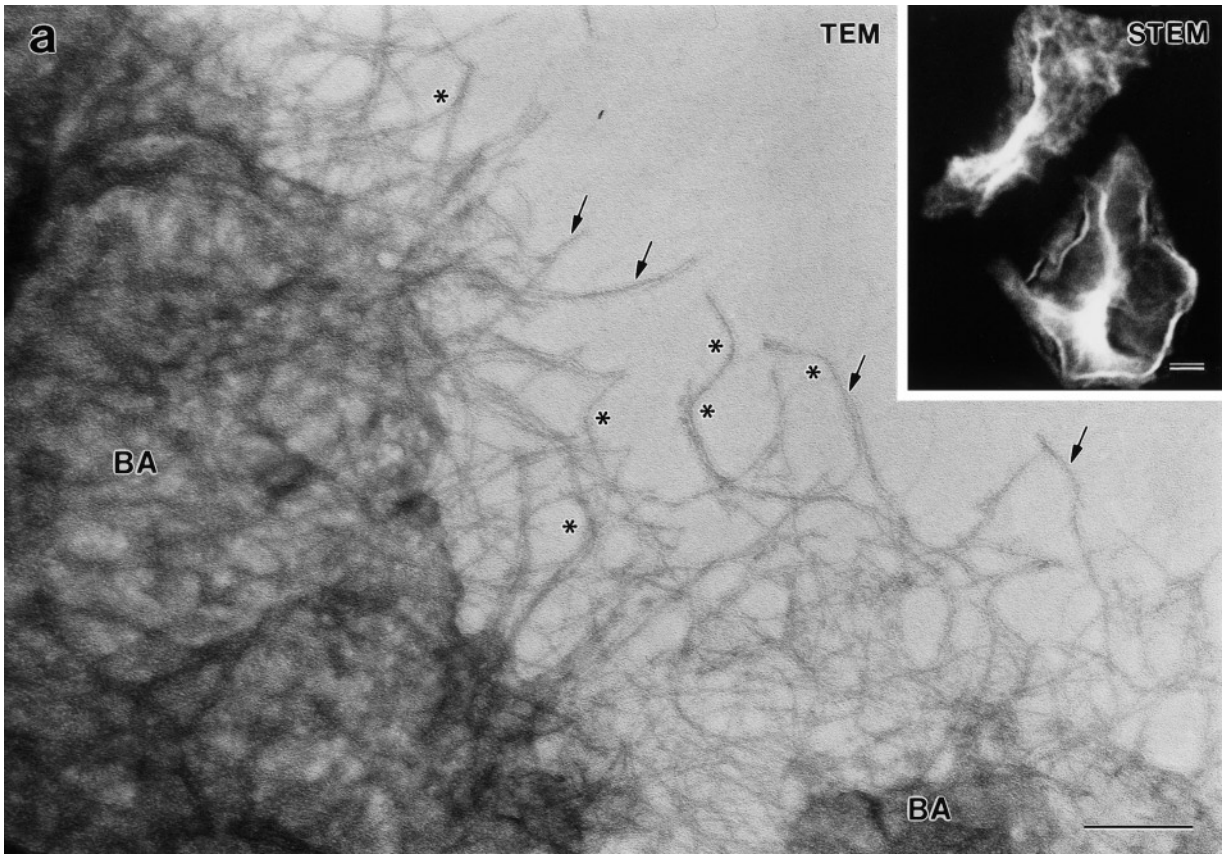

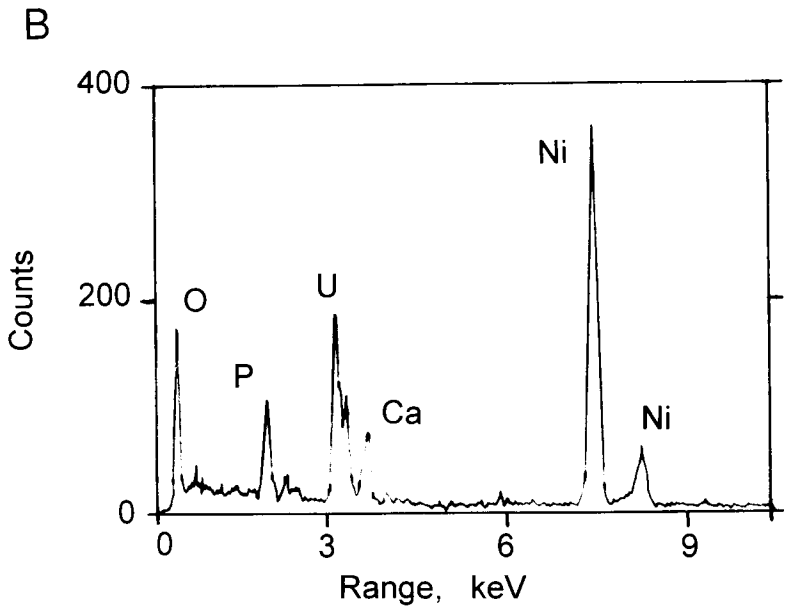

Fig. 8. Electron microscopic analyses of macromolecular complexes of BAG-75. **a:** Transmission electron micrograph illustrating ultrastructural detail of BAG-75 complexes formed in vitro as described in Methods. Complexes are visualized as roughly spherical, collapsed masses of protein. Each complex consists of a dense mat of multiple, overlapping fibrils forming the bulk of the aggregate (BA), and a peripheral fringe in which individual and composite strands of fibrillar protein can be readily observed (*arrows*). Extensive bending of individual fibrils is indicated by asterisks. Bar = 0.1 µm. **inset:** Low magnification STEM image of two individual aggregate structures. Bar = 1 µm. **b:** X-ray microanalysis of macromolecular BAG-75 complexes reveals elevated content of associated calcium and phosphorus atoms. This representative spectrum was generated from the uppermost aggregate structure depicted in the inset of panel a.

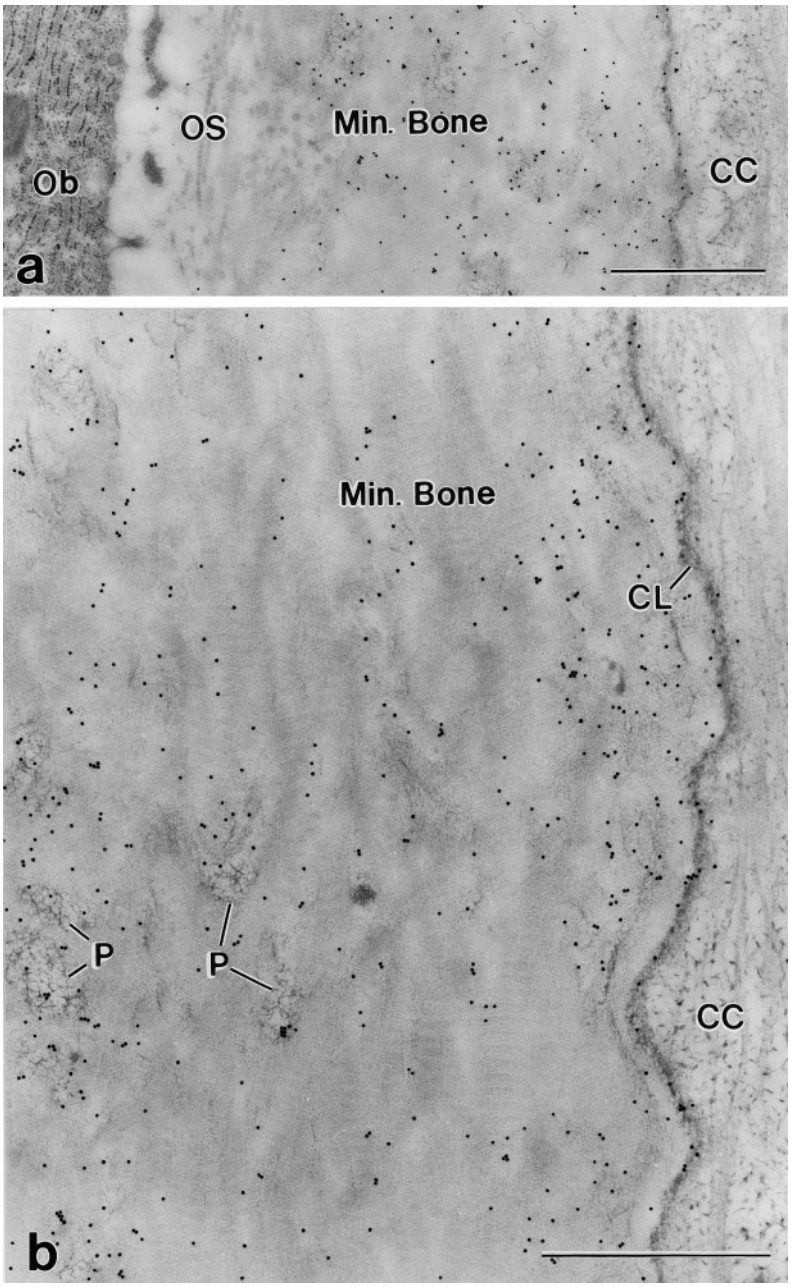

Fig. 9. Ultrastructural distribution of BAG-75 in bone but not cartilage of rat growth plate. Electron micrographs depicting bone formation in the primary spongiosa underlying the tibial growth plate after immunocytochemistry for BAG-75 using the postembedding, protein A-gold technique. **a:** Specific immunolabeling for BAG-75 is visualized as numerous gold particles primarily distributed over the mineralized bone (Min. Bone) compartment (here observed in a decalcified section). Relatively little labeling is observed over osteoid (OS) and calcified cartilage (CC). Ob, osteoblast. Bar = 1 μm. **b:** At higher magnification, immunolabeling for BAG-75 is dispersed among the collagen fibrils of mineralized bone (Min. Bone), and gold particles often appear to be somewhat linearly arranged. Reticulated patches (P) of organic matrix, known to be enriched in other bone phosphorproteins such as OPN and BSP, do not show an accumulation of BAG-75. Calcified cartilage (CC) is not labeled, although a few gold particles appear to be associated with the cement line (CL) found at the bone-calcified cartilage interface. Bar = 1 μm.

Sato et al. [1992] were the first to show by low angle platinum shadowing and TEM that purified BAG-75 can self-associate into microfibrils with an average diameter of 26.7 nm and lengths up of 1,000 nm. In a functional sense, osteoclasts appeared to preferentially respond to these large macromolecular complexes of BAG-75. Complexes of BAG-75 adsorbed onto bone surfaces functioned as effective inhibitors of bone resorption by rat or chicken osteoclasts [Sato et al., 1992]. Despite the use of several different methods, no evidence for direct binding of monomeric BAG-75 to osteoclasts could be obtained. The present study expands upon these initial findings in several key ways. First, monoclonal antibody HTP IV-#1 was produced by immunization of mice with complexes of BAG-75. Characterization by Western blotting and ELISA with purified BAG-75 and fractions from an ion exchange chromatogrpahic separation of a calvarial G/E extract demonstrated that MoAb HTP IV-#1 recognizes a neoepitope preferentially expressed on complexes of BAG-75 as compared with monomeric BAG-75. Second, using MoAb HTP IV-#1, we document for the first time the existence of complexes of BAG-75 in vivo in neonatal rat growth plate. Interestingly, complexes of BAG-75 were distributed focally and corresponded with areas of hydroxyapatite deposition; however, this association was not exclusive since BAG-75 complexes were also identified in nonmineralizing micromasses of osteoblastic ROS 17/2.8 cells.

Independent confirmation for macromolecular BAG-75 complexes in cells/tissues was obtained with immunoprecipitates of ^{3}H-leucine–labeled bone explant cultures using a separate, anti-BAG-75 peptide antibody (#503). After gel electrophoresis, immunoprecipitated BAG-75 radioactivity was located mostly at the top of the running gel, with a lesser amount migrating as a singlet (growth plate) or doublet (calvaria) band of approximately Mr = 200 kDa. The fact that similar sized complexes can be generated with purified BAG-75 in vitro [Gorski et al., in press] further supports the identity of immunoreactive bands >75 kDa as homologous or heterologous complexes of monomeric BAG-75. That biosynthetically labeled BAG-75 complexes are immunoprecipitated from explant cultures but not monolayer cultures [Gorski et al., 1990] and moreover are resistant to further dissociation suggests that the former complexes could be stabilized by intermolecular crosslinking catalyzed by tissue transglutaminase. Transglutaminase was shown by Aeschlimann et al. [1993] to be localized extracellularly in the lower hypertropic zone of the growth plate and in the calcified cartilage cores of the primary spongiosa. OPN [Prince et al., 1991; Beninati et al., 1994] and osteonectin [Aeschlimann et al., 1993] serve as substrates for tissue transglutaminase, and immunoblotting of bone extracts revealed high molecular weight complexes which were suggested to arise from transglutaminase-mediated crosslinking [Sorensen et al., 1994]. According to this rationale, polarized matrix deposition of BAG-75 by osteoblasts in explant cultures, as opposed to release into the media in monolayer cultures, would facilitate its concentration-dependent complexation and crosslinking by transglutaminase. Although the exact composition of BAG-75 complexes from bone is unknown, the fact that macromolecular complexes were found to copurify with monomeric BAG-75 or its Mr = 50 kDa fragment during ion-exchange chromatography indicates that the net charge properties of these forms are similar. Several additional controls suggest that formation of macromolecular complexes is a property of BAG-75 related to bone formation in situ. First, immunoprecipitates with anti-OPN antibodies from the same tissue extracts contained only an expected Mr = 50 kDa species and a characteristic fragment [Zhang et al., 1990]. Second, initial G/E extracts of explants were exchanged into radioimmunoassay buffer containing nonionic detergents and SDS [Gorski et al., 1990] which led to recovery of >90–95% of macromolecular radioactivity in the 100,000g × 1 h supernatants used for immunoprecipitations. This protocol greatly reduces nonspecific interactions. Finally, immunoblotting studies with neonatal calvarial and growth plate G/E extracts and anti-BAG-75 antibody (#504) detected monomeric BAG-75 and/or a Mr = 50 kDa fragment as well as complex bands near Mr = 200 kDa and at the top of the gel. This result demonstrates operationally that these BAG-75 forms and complexes are present within mineralized matrix. Since only biosynthetically labeled BAG-75 complexes were recovered from explant cultures, the presence of monomeric unlabeled BAG-75 in extracts may reflect the effect of local matrix factors and environment on self-association of BAG-75. For example, a low rate of osteoblastic synthesis or a looser

matrix with increased diffusion at earlier stages in development would be expected to yield more monomeric forms than that with a higher synthetic rate and/or reduced diffusion.

All preparations of BAG-75 analyzed thus far contain millimolar concentrations of phosphate. While it is likely that phosphate originates with the 0.35 M phosphate solution used to elute BAG-75 from hydroxyapatite during the last step of its purification, retention of phosphate ions by BAG-75 may reflect its physiological function in bone. Reproducible mineralization of osteoblastic cell cultures frequently requires inclusion of 5–10 mM beta-glycerol phosphate or another phosphate source in the culture media [Hunter et al., 1993]. Even in the presence of beta-glycerol phosphate, only interior regions of multilayer cultures are found to mineralize [Gerstenfeld et al., 1990; Lee et al., 1992]. The mechanism of action appears to require alkaline phosphatase–mediated release of inorganic phosphate [Hunter et al., 1993], which then participates directly in apatite formation. Such a mechanism implies that addition of beta-glycerol phosphate allows osteoblasts in in vitro culture systems to increase the local concentration of inorganic phosphate. Alternatively, normal mechanisms to concentrate phosphate operative in vivo may not function in in vitro culture systems.

Noncollagenous and plasma proteins in bone have been suggested to act as nucleators or as regulators of the growth of the apatitic crystals [Glimcher, 1989; Gorski, 1992; Hunter and Goldberg, 1994; Boskey, 1995]. A requisite corollary for such a role is presumed to be a close physical association with the earliest sites of mineralization. Using histochemical methods, Bonucci and others [Bonucci, 1967; Groot, 1982; Takagi, et al., 1983; Bonucci et al., 1988] demonstrated previously the existence of an acidic, filamentous, glycoproteinaceous phase (e.g., crystal ghost) in early "mineralization nodules" which shares the same shape, arrangement, and orientation as the inorganic crystallites. Recent immunocytochemical studies have documented in detail the precise distribution of a number of noncollagenous extracellular matrix and plasma proteins in relation to the mineral phase and collagen of bone [Bianco et al., 1993; Ingram et al., 1993; McKee et al., 1993; McKee and Nanci, 1995]. During embryonic development of bone, OPN, osteocalcin, BSP and α_2HS-glycoprotein colocalize with small mineralization foci within the osteoid and then later with irregular, dense "patches" of mineralized organic material apparently analogous to crystal ghosts. Serum components albumin and fibronectin do not follow this pattern and, at the ultrastructural level, seem to be more diffusely distributed throughout the mineralized bone matrix [reviewed in McKee and Nanci, 1993]. In vivo and in vitro data presented here place BAG-75 in the latter category. Although it is well known that OPN, BSP, and BAG-75 all bind strongly to the mineral phase in bone and thus should colocalize at similar sites of mineralization, the unique assembly of BAG-75 into fibrillar aggregates in vitro, independent of other proteins and mineral, implies a hierarchical order for matrix assembly and mineralization in vivo that may include creation of a supramolecular structure capable of spanning relatively large distances in bone. Consistent with its spherical matrix distribution surrounding osteoblasts in the primary spongiosa, an electronegative, three-dimensional BAG-75 network physically enveloping other noncollagenous proteins and collagen could serve an organizational role in forming bone or as a barrier restricting local diffusion of phosphate ions, thus facilitating establishment of regional ion concentration gradients. In an analogous way, type X collagen was proposed to form a barrier to limit mineralization of eggshell membranes [Arias et al., 1991], and tenascin appears to delineate the boundaries of individual barrel fields during formation of the rodent somatosensory cortex [Mitrovic et al., 1994].

ACKNOWLEDGMENTS

Continued support of this research by Drs. Ron MacQuarrie and Marino Martinez-Carrion is acknowledged. J.P.G. thanks Mrs. Kathy Huntoon and Lisa Luetmer for excellent technical assistance; the authors thank I. Turgeon and S. Zalzal (Montreal) for their technical help in tissue processing for immunochemistry and for the preparation of protein A-gold complex, respectively, and Dr. L. Peru (Montreal) for help with the X-ray microanalysis. The help of Tom Beito and Dr. Chris Krco (Mayo Clinic, Rochester, MN) in preparation of monoclonal antibodies against BAG-75 is gratefully acknowledged; the help of Dr. Tom Moyer (Mayo Clinic) with calcium measurements is greatly appreciated. Grant support was provided by NIH grants AR37078 and AR40923 (J.P.G.), by

the Scientific Education Partnership (J.P.G.), by the Orthopedic Research and Education Foundation (J.P.G.), by a UMKC faculty research grant (J.P.G.), by an institutional NIH biomedical support grant (J.P.G.), by an American Society for Biochemistry and Molecular Biology high school teacher summer fellowship (S.R. and J.P.G.), by the Medical Research Council of Canada (M.D.M.), and by the FRSQ of Quebec (M.D.M.).

REFERENCES

Aeschlimann D, Wetterwald A, Fleisch H, Paulsson M (1993): Expression of tissue transglutaminase in skeletal tissues correlates with events of terminal differentiation of chondrocytes. J Cell Biol 120:1461–1470.

Arias AL, Fernandez MS, Dennis JE, Caplan AI (1991): Collagens of the chicken eggshell membranes. Connect Tissue Res 26:37–45.

Barlett GR (1959): Phosphorus assay in column chromatography. J Biol Chem 234:466–468.

Baron R (1993): Anatomy and Ultrastructure of Bone. In Favus MJ (ed): "Primer on the Metabolic Bone Diseases and Disorders of Mineral Metabolism." New York: Raven Press, pp 3–9.

Bendayan M (1989): Protein A-gold and protein G-gold postembedding immunoelectron microscopy. In Hayat MA (ed): "Colloidal Gold: Principles, Methods, and Applications," Vol 1. New York: Academic Press, pp 33–94.

Beninati S, Senger DR, Cordella Miele E, Mukherjee AB, Chackalaparampil I, Shanmugam V, Singh K, Mukherjee BB (1994): Osteopontin: Its tranglutaminase-catalyzed posttranslational modifications and cross-linking to fibronectin. J Biochem 115:675–682.

Bianco P, Riminucci M, Silvestrini G, Bonucci E, Termine JD, Fisher LW, Gehron Robey P (1993): Localization of bone sialoprotein (BSP) to Golgi and post-Golgi secretory structures in osteoblasts and to discrete sites in early bone matrix. J Histochem Cytochem 41:193–203.

Bonucci E (1967): Fine structure of early cartilage calcification. J Ultrastruct Res 20:33–50.

Bonucci E, Silvestrini G, Di Grezia R (1988): The ultrastructure of the organic phase associated with the inorganic substance in calcified tissues. Clin Ortho Rel Res 233:243–261.

Boskey AL (1995): Osteopontin and related phosphorylated sialoproteins: Effects on mineralization. Ann N Y Acad Sci 760:249–256.

Boskey AL, Maresca M, Ullrich W, Doty SB, Butler WT, Prince CW (1993): Osteopontin-hydroxyapatite interactions in vitro: Inhibition of hydroxyapaptite formation and growth in a gelatin-gel. Bone Miner 22:147–159.

Bumol TF, Walker LE, Reisfeld RA (1984): Biosynthetic studies of proteoglycans in human melanoma cells with a monoclonal antibody to a core glycoprotein of chondroitin sulfate proteoglycans. J Biol Chem 259:12733–12741.

Chen Y, Bhajanit BS, Gorski JP (1992): Calcium and collagen binding properties of osteopontin, bone sialoprotein, and bone acidic glycoprotein-75 from bone. J Biol Chem 267:24871–24878.

Fazekas de St Groth S, Scheidegger D (1980): Production of monoclonal antibodies: strategy and tactics. J Immunol Methods 35:1–21.

Fisher LW, McBride OW, Termine JD, Young MF (1990): Human bone sialoprotein: Deduced protein sequence and chromosomal localization. J Biol Chem 265:2347–2351.

Gerstenfeld LC, Gotoh Y, McKee MD, Nanci A, Landis WJ, Glimcher MJ (1990): Expression and ultrastructural localization of a major 66 kDa phosphoprotein synthesized by chicken osteoblasts during in vitro mineralization. Anat Rec 228:93–103.

Glimcher MJ (1989): Mechanisms of calcification: Role of collagen fibrils and collagen-phosphoprotein complexes in vitro and in vivo. Anat Rec 224:139–153.

Gorski JP (1992): Acidic phosphoproteins from bone matrix: A structural rationalization of their role in biomineralization. Calcif Tissue Int 50:391–396.

Gorski JP, Shimizu K (1988): Isolation of new phosphorylated glycoprotein from mineralized phase of bone that exhibits limited homology to adhesive protein osteopontin. J Biol Chem 263:15938–15945.

Gorski JP, Griffin D, Dudley G, Stanford C, Thomas R, Huang C, Lai E, Karr B, Solursh M (1990): Bone acidic glycoprotein-75 is a major synthetic product of osteoblastic cells and localized as 75- and/or 50-kDa forms in mineralized phases of bone and growth plate and in serum. J Biol Chem 265:14956–14963.

Gorski JP, Kremer E, Ruiz-Perez J, Wise GE, Artigues A (1995): Conformational analyses on soluble and surface bound osteopontin. Ann N Y Acad Sci 760:12–23.

Gorski JP, Kremer E, Chen Y (1996): Bone acidic glycoprotein-75 self-associates to form large macromolecular complexes. Connect Tissue Res 35:136–144.

Gotoh Y, Pierschbacher MD, Grzesiak JJ, Gerstenfeld L, Glimcher MJ (1990): Comparison of two phosphoproteins in chicken bone and their similarities to the mammalian bone proteins, osteopontin and bone sialoprotein II. Biochem Biophys Res Commun 173:471–479.

Groot CG (1982): An electron microscopic examination for the presence of acid groups in the organic matrix of mineralization nodules in foetal bone. Metab Bone Dis Rel Res 4:77–84.

Helfrich MH, Nesbitt SA, Dorey EL, Horton MA (1992): Rat osteoclasts adhere to a wide range of RGD peptide-containing proteins, including the bone sialoproteins and fibronectin, via a beta-3 integrin. J Bone Miner Res 7:335–343.

Heinegard D, Oldberg A (1989): Structure and biology of cartilage and bone matrix noncollagenous macromolecules. FASEB J 3:2042–2051.

Hunter GK, Goldberg HA (1994): Modulation of crystal formation by bone phosphoproteins: role of glutamic acid–rich sequences in the nucleation of hydroxyapatite by bone sialoprotein. Biochem J 302:175–179.

Hunter GK, Holmyard DP, Pritzker KP (1993): Calcification of chick verbebral chondrocytes grown in agarose gels: A biochemical and ultrastructural study. J Cell Sci 104:1031–1038.

Hunter GK, Kyle CL, Goldberg HA (1994): Modulation of crystal formation by bone phosphoproteins: Structural specificity of the osteopontin-mediated inhibition of hydroxyapatite formation. Biochem J 300:723–728.

Ingram RT, Clarke BL, Fisher LW, Fitzpatrick LA (1993): Distribution of noncollagenous proteins in the matrix of

adult human bone: Evidence of anatomic and functional heterogeneity. J Bone Miner Res 8:1019–1029.

Jee, WSS (1983): The skeletal tissues. In Weiss L (ed): "Histology: Cell and Tissue Biology." New York: Elsevier Biomedical, pp 200–255.

Lee KL, Aubin JE, Heersche JN (1992): Beta-glycerol phosphate induced mineralization of osteoid cells does not alter expression of extracellular matrix components in fetal rat calvarial cultures. J Bone Miner Res 7:1211–1219.

Lowenstam A, Weiner S (1989): Biomineralization processes. In: "On Biomineralization." London: Oxford University Press, pp 25–49.

Magnuson SK, Booth R, Porter S, Gorski JP (1997): Bilateral tibial marrow ablation induces a transient hypercalcemia arising from a wave of systemic bone resorption inhibitable with methylprednisolone or deflazacort. J Bone Miner Res 12.

McKee MD, Nanci A, Landis WJ, Gotoh Y, Gerstenfeld LC, Glimcher MJ (1990): Developmental appearance and ultrastructural immunolocalization of a major 66 kDa phosphoprotein in embryonic and post-natal chicken bone. Anat Rec 228:77–92.

McKee MD, Nanci A (1993): Ultrastructural, cytochemical and immunocytochemical studies on bone and its interfaces. Cells Mater 3:219–243.

McKee MD, Farach-Carson MC, Butler WT, Hauschka PV, Nanci A (1993): Ultrastructural immunolocalization of noncollagenous (osteopontin and osteocalcin) and plasma (albumin and α_2HS-glycoprotein) proteins in rat bone. J Bone Miner Res 8:485–496.

McKee MD, Nanci A (1995): Postembedding colloidal-gold immunocytochemistry of non-collagenous extracellular matrix proteins in mineralized tissues. Microsc Res Tech 31:44–62.

Mitrovic N, Dorries U, Schachner U (1994): Expression of the extracellular matrix glycoprotein tenascin in the somatosensory cortex of the mouse during postnatal development: An immunocytochemical and in situ hybridization analysis. J Neurocytol 23:364–378.

Oldberg A, Franzen A, Heinegard D (1986): Cloning and sequence analysis of a rat bone sialoprotein (osteopontin) cDNA reveals an Arg-Gly-Asp cell binding sequence. Proc Natl Acad Sci U S A 83:8819–8823.

Oldberg A, Franzen A, Heinegard D (1988a): The primary structure of a cell-binding bone sialoprotein. J Biol Chem 263:19430–19432.

Oldberg A, Franzen A, Heinegard D, Pierschbacher M, Ruoslahti E (1988b): Identification of a bone sialoprotein receptor in osteosarcoma cells. J Biol Chem 263:19433–19436.

Pinto MR, Gorski JP, Penniston JT, Kelly PJ (1988): Age-related changes in composition and Ca^{2+}-binding capacity of canine cortical bone extracts. Am J Physiol 255: H101–H110.

Prince CW, Dickie D, Krumdieck CL (1991): Osteopontin, a substrate for transglutaminase and factor XIII activity. Biochem Biophys Res Commun 177:1205–1210.

Ritter MN, Farach-Carson MC, Butler WT (1992): Evidence for the formation of a complex between osteopontin and osteocalcin. J Bone Miner Res 7:877–885.

Ross FP, Chappel J, Alvarez JI, Sander D, Butler WT, Farach-Carson MC, Mintz KA, Gehron-Robey P, Teitelbaum SL, Cheresh DA (1993): Interactions between the bone matrix proteins osteopontin and bone sialoprotein and the osteoclast integrin $\alpha_5\beta_3$ potentiate bone resorption. J Biol Chem 268:9901–9907.

Sato, M. Grasser W, Harms S, Fullenkamp C, Gorski JP (1992): Bone acidic glycoprotein-75 inhibits resorption activity of isolated rat and chicken osteoclasts. FASEB J 6:2966–2976

Solursh M, Meier S (1972): The requirement for RNA synthesis in the differentiation of cultured chick chrondocytes. J Exp Zool 181:253–262.

Somerman MJ, Fisher LW, Foster RA, Sauk JJ (1988): Human bone sialoprotein I and II enhance fibroblast attachment in vitro. Calcif Tissue Int 43:50–53.

Sorensen ES, Rasmussen LK, Moller L, Jensen PH, Hojrup P, Petersen TE (1994): Localization of transglutaminase-reactive glutamine residues in bovine osteopontin. Biochem J 304:13–16.

Takagi M, Parmley RT, Toda Y, Denys FR (1983): Ultrastructural cytochemistry of complex carbohydrates in osteoblasts, osteoid, and bone matrix. Calcif Tissue Int 35:309–319.

Weiner S, Traub W (1992): Bone structure: From angstroms to microns. FASEB J 6:879–885.

Zhang Q, Domenicucci C, Goldberg H, Wrana JL, Sodek J (1990): Characterization of fetal porcine bone sialoproteins, secreted phosphoprotein I (SPP1, osteopontin), bone sialoprotein, and a 23 kDa glycoprotein. J BiolChem 265:7583–7589.